Oscillations of electrical conductivity in single bismuth nanowires

T. W. Cornelius,[1,*] M. E. Toimil-Molares,[1] S. Karim,[2] and R. Neumann[1]
[1]*Gesellschaft für Schwerionenforschung (GSI), Planckstrasse 1, D-64291 Darmstadt, Germany*
[2]*Department of Chemistry, Philipps University Marburg, Hans-Meerwein-Strasse, D-35032 Marburg, Germany*
(Received 24 August 2007; revised manuscript received 8 October 2007; published 26 March 2008)

Bismuth nanowires were electrochemically deposited in ion track-etched polycarbonate membranes. Single wires with diameters ranging between 70 and 550 nm were created in membranes with one single nanopore and their electrical resistance was investigated while leaving them embedded in the template. The specific electrical conductivity oscillates as a function of wire diameter. The modulations are discussed on the basis of quantum-size effects which lead to a splitting of the energy bands into subbands and, thus, cause an oscillation of the density of states at the Fermi level depending on the diameter.

DOI: 10.1103/PhysRevB.77.125425 PACS number(s): 73.63.−b, 72.20.−i

INTRODUCTION

In recent years, the electrical transport properties of nanoscaled objects raised enormous interest. Several studies focused on classical size effects occurring in objects of dimensions comparable with the electron mean free path l_e. Detailed models have been established,[1–3] and some predictions have been confirmed by experimental results on bismuth nanowires. Bismuth exhibits unique electronic properties, such as extremely small electron effective mass m^* ($10^{-3}m_e$ depending on the crystalline direction[4]), highly anisotropic Fermi surface, and long l_e [$\sim$100 nm at room temperature (RT)[5]]. Because of the minute m^* and the large Fermi wavelength λ_F (40–70 nm at RT[6,7]), Bi nanowires are excellent objects for studies on how quantum confinement influences the electronic properties of quasi-one-dimensional (quasi-1D) systems. Further, bismuth is a semimetal with a very small band overlap ($E_0 \sim 38$ meV at 0 K). The Fermi energy in bismuth is only $E_F \sim 56$ meV at room temperature.[8] Electrons and holes are located at the L point and at the T point of the Brillouin zone, respectively. The charge carrier density n amounts to only 3×10^{18} cm^{-3} at RT and decreases by 1 order of magnitude when cooling Bi down to liquid helium temperature.

When the object size is comparable to λ_F, quantum-size effects (QSEs) are expected to occur.[9] QSEs cause a splitting of the energy bands in subbands and, consequently, a shift of the band edges away from each other [Fig. 1(a)]. Due to the subband splitting, the electronic density of states (DOS) at the Fermi level changes [Fig. 1(b)] and, thus, the two-dimensional quantum confinement of the resulting quasi-one-dimensional electron gas in nanowires provides a method to manipulate the electronic transport properties of the material. This gives rise to utilizing the electronic transport properties of various quasi-1D material systems for a wide range of practical devices. For instance, Bi and its alloys are regarded as promising candidates for future thermoelectric nanodevices. In bulk materials, the parabolic DOS means that the electron density around the Fermi level is small, while in nanowires, the spikes in the DOS suggest that the thermoelectric power factor can be increased and, thus, the thermoelectric performance can be improved.

Furthermore, the band shift involves a decrease of the band overlap E_0, implying that a critical diameter d_c exists for which the band overlap vanishes and, as a consequence, the nanowires undergo a transition from a semimetal to a semiconductor.[4] In a previous study, we found an infrared absorption whose edge is blueshifted with decreasing wire diameter, which was attributed to a shift of the band edges caused by QSE.[10]

In this work, we report electrical conductivity oscillations in bismuth nanowires with diameters between 70 and 550 nm, which are caused presumably by subband splitting arising from QSE. To our knowledge, modulations in electrical transport characteristics were detected for thin films,[7,11] however, until now not found in nanowires. This can be understood by the fact that most experiments were performed

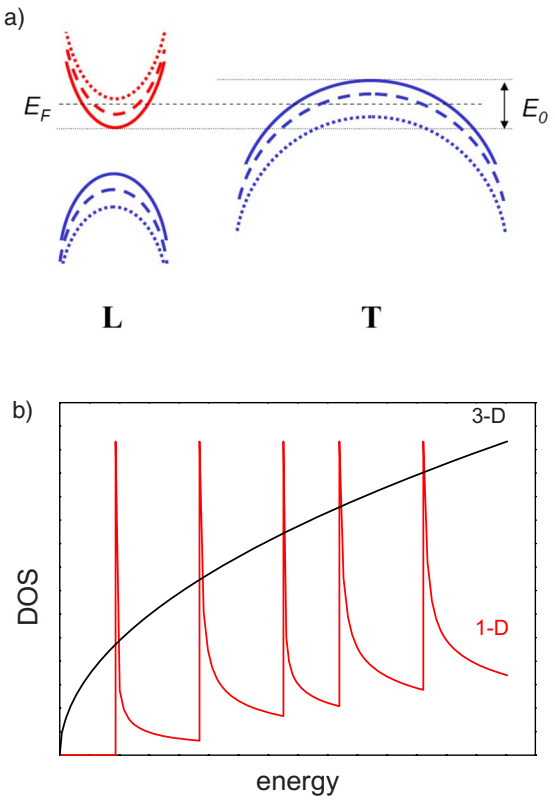

FIG. 1. (Color online) (a) Schematic of the three-band model of bismuth including the subband splitting caused by QSE. (b) Density of states for three- and one-dimensional materials.

on nanowire arrays[12–15] prohibiting the determination of absolute resistance and, thus, of the specific electrical conductivity for a single wire. Up to now, only few studies deal with single wires. In Ref. 5, Cronin *et al.* reported the fabrication of wire arrays by pressure injection in alumina templates and the subsequent removal of the matrix with a strong acid. Though a single wire was contacted lithographically, reliable contacting failed due to the presence of a modified surface layer forming during matrix dissolution. Further, single wires consisting of very small grains were prepared and contacted by an electron-beam writing technique on a Si substrate.[16] However, in order to detect quantum-size effects, the degree of crystalline quality of the wire plays a crucial role. In addition to the condition of size quantization, $\lambda_F \sim d$, it is necessary that l_e exceeds d. If the grains of the wire are too small, the electrons are scattered predominantly from grain boundaries and QSE will be suppressed.

EXPERIMENT

Single bismuth nanowires were grown electrochemically in polycarbonate (Makrofol N, Bayer) membranes of 30 μm thickness containing one single nanopore. Single-pore membranes are produced by irradiating polymer foils with a single swift heavy ion at the UNILAC linear accelerator of GSI through a mask with an aperture of 200 μm and subsequent chemical etching. The ion beam is defocused in such a way that approximately 1 ion/s penetrates the sample. A semiconductor detector, placed behind the sample, records every ion passing through the foils, and by using an electrostatic beam chopper, the irradiation is stopped within 10 μs. This method allows the irradiation of foils with a selected number of ions, ranging from one to several hundred.[17] The damage trail along the ion trajectory was chemically etched in 2*M* NaOH at 60 °C producing a cylindrical channel. The pore diameter of a given membrane was determined by measuring the electrical current through the nanopore employing a 1*M* KCl solution and two Ag/AgCl electrodes. The effective pore diameter d_{eff} was calculated by applying the following equation:

$$d_{\text{eff}} = \sqrt{\frac{4L}{\sigma_{\text{KCl}}\pi}\frac{I}{U}}. \quad (1)$$

Here, L is the pore length corresponding to the membrane thickness, σ_{KCl} denotes the conductivity of the 1*M* KCl solution (10 S/m at 20 °C), U is the applied potential, and I is the measured electrical current.

Before electrochemical filling, a gold coating was sputtered on one side of the membrane which was reinforced by an electrochemically deposited copper layer. A single bismuth nanowire was electrochemically grown in the nanopore applying −25 mV at 50 °C.[18] The deposition was continued until a cap was formed on top of the wire. In order to contact the wire electrically, the cap was coated by an additional gold layer that was sputtered on top. For electrical measurements, the whole sample (membrane with embedded wire) was placed between two macroscopic copper plates with the cap being protected from direct pressure by a caved upper electrode (see Fig. 2).[19,20] The contact resistances were neglected because of the high resistance of the wire itself.

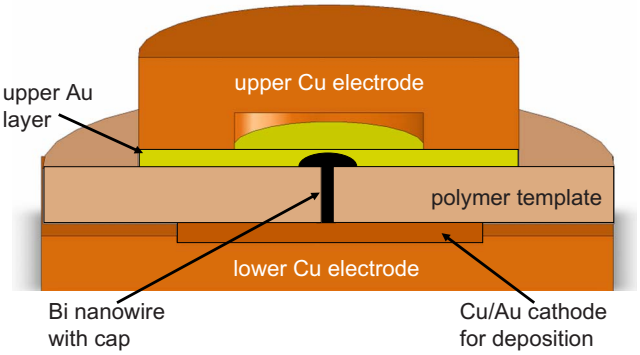

FIG. 2. (Color online) Schematic of the electrical contacting of a single nanowire embedded in the template.

When studying the electrical transport properties of nanostructures, in particular, quantum-size effects, both their morphology and crystallinity are of great importance. These two characteristics were investigated by preparing arrays of nanowires in multipore templates under the same conditions as single wires. Subsequently, the templates were dissolved in dimethylformamide and the needles were studied by scanning (Philips XL 30) and transmission electron microscopies (TEM) (Philips CM 20). For the TEM examinations, the wires were detached from the backing electrode. For this purpose, the beaker containing the solvent with the sample was introduced after template dissolution in an ultrasonic bath. Thereafter, few drops of the wire suspension were put on a carbon-covered TEM grid.

RESULTS AND DISCUSSION

During the electrochemical deposition of bismuth in multipore as well as single-pore templates, the current transient was recorded, as displayed in Figs. 3(a) and 3(b), respectively. The *I-t* curves exhibit three sections. (I) At the very beginning of the deposition, a current peak is observed which is much less pronounced in the case of a single wire than for arrays. It originates from an electrical double layer at the metal-electrolyte interface which is discharged during the very first seconds of the process. Subsequently, (II) the deposition current remains constant for a longer period of time, (III) until it starts to increase and finally saturates. In the case of potentiostatic depositions, the current density j, i.e., current per area ($j=I/A$), is constant. Therefore, a steady current is recorded during deposition in cylindrical pores. The deposition current for single wires with diameter of a few hundreds of nanometers amounts to less than 100 pA. As soon as the metal reaches the opposite side of the membrane and the deposition process is no longer restricted to the pore geometry, a cap is formed on top of the wire. The start of the cap growth becomes apparent by a significant increase of the current due to both a larger deposition area during cap formation and a constant current density. This current rise is much more pronounced for single-wire depositions where the current increases by 3–4 orders of magnitude within less

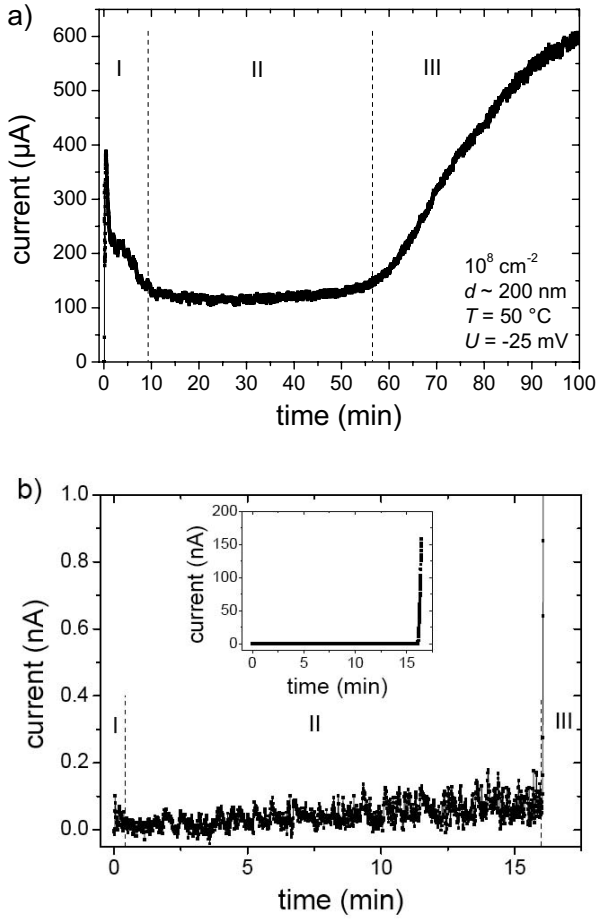

FIG. 3. Current vs time curves for the deposition of (a) 10^8 wires/cm^2 and (b) a single nanowire applying −25 mV at 50 °C.

than a minute [see the inset of Fig. 3(b)]. Since the current is a function of the deposition area, the current gain indicates that the size of the cap grown on top of a single wire is up to hundred times larger than the wire diameter, i.e., of the order of 10 μm for a 100 nm wire. In turn, this sudden current increase is a clear indication that the pore was completely filled by the metal.

From the deposited charge Q, which is obtained by integrating the area beneath the I-t curve for a single-pore membrane before the cap growth, the filled volume V can be calculated using Faraday's law,

$$Q = \frac{Ze}{Am_u}\rho V. \tag{2}$$

Here, Z is the ion charge, e is the elementary charge, A is the number of nucleons contained in the ion, m_u is the proton mass, and ρ is the density of the deposited material. Assuming a cylindrical geometry of the nanowire, its diameter can be computated from the filled volume. For the deposition shown in Fig. 3(b), the deposited charge amounts to 42.4 ± 0.3 nC equivalent to a wire diameter of 366 ± 15 nm. This is in good accordance with the result of the conductometric measurement in KCl on the as-prepared single nanopore with an effective pore diameter of 355 ± 22 nm. Hence, the deposited Bi nanowire completely fills the nanopore, evidencing that the conductivity measurement using KCl is an appropriate tool to determine the pore and, in turn, the wire diameter.

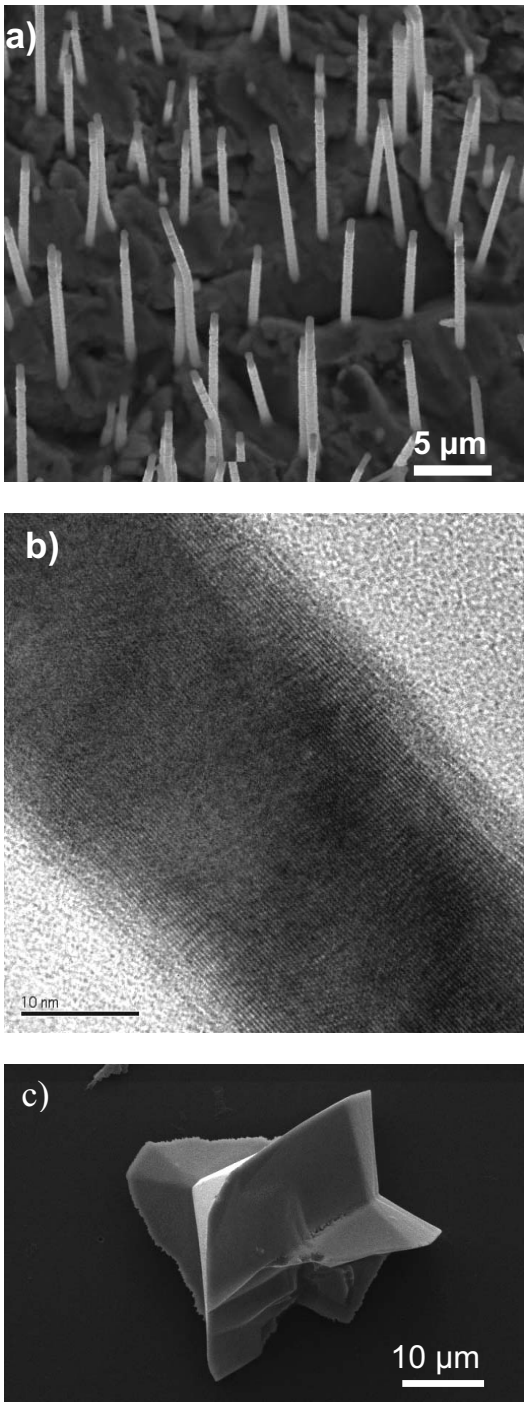

FIG. 4. (a) Scanning electron microscopy image of freestanding bismuth nanowires with 400 nm diameter. (b) High-resolution transmission electron micrograph of a bismuth nanowire with 30 nm diameter. (c) Scanning electron microscopy image of a cap grown on top of a single Bi nanowire.

Figure 4(a) displays a scanning electron microscopy image of freestanding bismuth nanowires revealing cylindrical

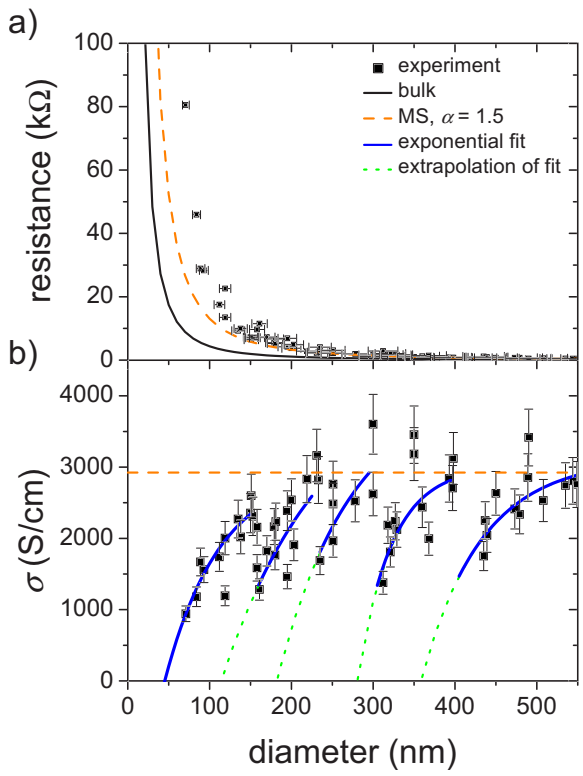

FIG. 5. (Color online) (a) Electrical resistance and (b) specific electrical conductivity of single bismuth nanowires as a function of diameter. The dashed curves take into account electron scattering at grain boundaries using the MS model. The solid and dotted lines in part (b) represent exponential fits using $\sigma=A+B\exp(-d/d_c)$ and their interpolation to $\sigma=0$.

needles with uniform diameter of ~400 nm along their complete length. These findings coincide with small-angle x-ray scattering results on ion track-etched polycarbonate membranes which demonstrated that our templates contain highly cylindrical nanopores,[21] in contrast to commercial membranes where cigar-shaped pores were found.[22] A high-resolution TEM micrograph of a wire with 30 nm diameter is presented in Fig. 4(b). The image shows the atomic lattice of the nanowire evidencing the high crystalline quality. The excellent wire quality (cylindricity and crystallinity) makes these wires ideally suited for studying electron transport in the frame of quantum-size effects. It is assumed that the structural properties of a single wire are the same as for wire arrays. This is supported by investigations of caps grown on top of single wires revealing that they contain large crystals [Fig. 4(c)].

The electrical resistance measurements of single bismuth nanowires with diameters ranging between 70 and 550 nm are displayed in Fig. 5(a). All wires show resistances significantly higher than the classically calculated value based on the resistivity of bulk bismuth ($\rho_{\text{bulk}}=114\ \mu\Omega$ cm); i.e., the data points of the nanowires are well above the solid curve. The smaller the wire diameter is, the larger the deviation gets. In a previous work, we showed that the discrepancy between the resistance of wires with $d>150$ nm and the bulk value can be ascribed to additional electron scattering from grain boundaries.[20] Mayadas and Shatzkes developed a model (MS model) in order to take additional electron scattering at grain boundaries into account, which is a function of a coefficient α being dependent on the electron mean free path, the mean grain size D, and the reflectivity of the grain boundaries $\mathcal{R}$,[2]

$$\frac{\rho_{\text{bulk}}}{\rho}=3\left[\frac{1}{3}-\frac{1}{2}\alpha+\alpha^2-\alpha^3\ln\left(1+\frac{1}{\alpha}\right)\right], \tag{3}$$

with $\alpha=(l_e/D)[\mathcal{R}/(1-\mathcal{R})]$.

The resistance as a function of d, employing this model and considering $\alpha=1.5$ ($\rho=3\rho_{\text{bulk}}$), is represented by the dashed curve which describes the data down to $d\sim150$ nm, much better than without taking into account any finite-size effects. These findings are in agreement with our previous results.[20] However, for smaller diameters, the data deviate toward larger resistances than predicted by this approach.

The specific electrical conductivity of the nanowires derived from the resistance as well as the conductivity calculated by means of the MS model are plotted in Fig. 5(b). The data reveal oscillations as a function of wire diameter that cannot be explained by mesoscopic effects. They can be described well by an exponential law corresponding to $\sigma=A+B\exp(-d/d_c)$, with A and B being fitting parameters, where A is related to the wire conductivity given by the MS model.

The specific electrical conductivity is a function of both the charge carrier density n and the mobility μ ($\sigma=ne\mu$). As already mentioned above, QSE causes a splitting of the energy bands in subbands and, thus, a shift of the band edges away from each other. The energy shift can be described by the following expression with N being the number of the subband:

$$\Delta E\approx\frac{N^2\hbar^2\pi^2}{m^*d^2}. \tag{4}$$

The number of subbands corresponds to discrete values of the wave vector along the "quantizing" dimensions of the nanowire. Owing to the spikelike DOS for nanowires, the kinetic properties of the system will oscillate as a function of d, as long as the carrier gas is degenerate. These oscillations are connected with abrupt changes of the density of states on the Fermi surface as one subband after another passes E_F. According to Sandormiskii[9] and Farhangfar,[23] the periodicity for films and rectangular nanowires is given by the critical thickness and width, respectively. Assuming that the Fermi level does not shift with the wire diameter, and according to Eq. (4), d_c is approximately given by

$$d_c\approx\frac{N\hbar\pi}{\sqrt{\Delta Em^*}}=\frac{Nh}{\sqrt{4E_Fm^*}}. \tag{5}$$

The electron effective mass is a function of the band gap. This function involves an increasing m^* with enlarging band gap because of strong coupling between conduction and valence bands at the L point which is represented by the matrix element $\langle v|p|c\rangle$. This strong coupling is taken into account by the Lax two-band model,[24,25] resulting in the following expression:

$$d_c \approx \frac{Nh}{\sqrt{4E_F m_e}} \sqrt{1 + \frac{2}{m_e}\frac{|\langle v|p|c\rangle|^2}{E_g} - \frac{12\hbar^2 k^2 |\langle v|p|c\rangle|^4}{E_g^3 m_e}}, \tag{6}$$

with m_e being the free electron mass.

As already mentioned, exponential curves can be fitted to the oscillations of the electrical conductivity vs wire diameter. The periodicity is extracted from the intersection points of the extrapolated fitting curves (represented by dotted lines) with the x axis. The first intersection point represents the critical diameter for the semimetal-semiconductor transition amounting to $d_c=40$ nm. Fitting Eq. (6) using $E_F=56$ meV (Ref. 8) to this experimental value, $m^*=0.0022m_e$ at the band edge ($k=0$) is derived for bulk Bi being a reasonable value for electrons at the L point.

Assuming a constant Fermi energy and taking into account only coupling between the Nth subband of the conduction band and the Nth subband of the valence band, the expression under the square root is the same for all subbands. Thus, the electron effective mass is the same for all levels when they pass the Fermi level and, in turn, the periodicity of the conductivity oscillations is a multiple of d_c. Though, the experimental periodicity does not follow this rule. The critical diameters amount to 40, 115, 182, 281, and 358 nm. This progression can be approximated by a $d_{c_n} \sim (n+1/2)d_0$, proportional with $d_0=80$ nm and n being a natural number including zero similar to the energy levels of a harmonic oscillator. This discrepancy may arise from at least three simplifications made for the computations above. (i) For the calculations, an infinitely deep rectangular potential well was assumed. However, the potential may be deformed by charge states located at the wire surface leading to a behavior as observed. For instance, Komnik *et al.* found surface defects which acted as additional charge carriers for bismuth thin films.[26] The surface charge density amounted to 2.75×10^{12} cm^{-2}. (ii) A constant Fermi energy was assumed. Besides the subband splittings of the electron bands at the L point, the bands at the T point, where the holes are located, split into separate energy levels. Due to the much larger mass of the holes compared to the electrons, the splittings at the T point are less pronounced than at the L point. However, it may affect the electron density and lead to a variable Fermi energy because of the charge neutrality principle. (iii) For the evaluation of Eq. (6), only the coupling between the Nth subband of the conduction band and the Nth subband of the valence band was taken into account. However, there may also be coupling to other subbands involving different electron effective masses for the different energy levels when passing E_F. Thus, the expression under the square root is not the same anymore for all subbands, which may lead to the observed periodicity.

The exponential behavior of the oscillations may be explained by the thermal excitation of charge carriers. Only charge carriers close to the Fermi level contribute to the electrical transport. When a subband passes E_F, it is depleted and the charge carriers are transferred to lower states. At RT, they are excited thermally to higher subbands so that they participate in the electrical transport. With increasing band gap, i.e., decreasing wire diameter, the number of thermally excited carriers decreases and, thus, the electrical conductivity drops. As soon as a lower subband approaches E_F, the charge carrier density recovers and, hence, the conductivity increases to about 3000 S/cm being in agreement with the mean resistivity of 440 $\mu\Omega$ cm ($\sigma=2272$ S/cm) reported in Ref. 20. The whole process occurs repeatedly until the lowest subband passed the Fermi level and the material is transferred into a semiconductor.

However, in order to observe QSE, two preconditions have to be satisfied. (i) The relaxation time τ must be sufficiently long, i.e., $\tau > \hbar/(E_{n+1}-E_n)$, with $(E_{n+1}-E_n)$ being the energy separation between two subbands at the Fermi level. (ii) The thermal broadening of the levels must be small compared to the subband splitting. In order to fulfil the first requirement, the specimens must consist of grains much larger than l_e and should possess only a small number of defects. As presented in the transmission electron microscopy image in Fig. 4(b), the wires exhibit very good crystalline structure. Moreover, the wire resistivity is only about three times larger than the bulk value, whereas Chiu and Shih[16] reported resistivities more than 20 times larger for wires with diameter of $\leq$200 nm than that for bulk Bi. Thus, we assume that the first requirement is fulfilled for the wires under study. In order to meet the second precondition, the subband splitting at the Fermi level must exceed 25 meV which corresponds to kT at 300 K. Such a large splitting seems to be unreasonable, especially, when taking into account that the first oscillation is observed for wires with $d\sim400$ nm. However, there are a number of studies reporting QSE at RT for Bi thin films with thicknesses of >100 nm.[7,11] Since nanowires confine the electronic wave function in two instead of only one dimension like in thin films, quantum-size effects are expected to occur at diameters larger than the reported film thicknesses.

CONCLUSION

In conclusion, single bismuth nanowires with diameters ranging between 70 and 550 nm were electrochemically fabricated in ion track-etched polycarbonate membranes. Their electrical conductivity as a function of diameter reveals an oscillatory behavior. There are reasonable arguments that these sharp periodic alterations originate from a modulation of the density of states at the Fermi level.

ACKNOWLEDGMENTS

The authors gratefully acknowledge M.S. Dresselhaus from MIT in Boston (USA) for valuable discussions. One of the authors (S.K.) expresses his gratitude for support from the Higher Education Commission (HEC) of Pakistan.

*Corresponding author. FAX: +49 (0)6159-712179; th.cornelius@gsi.de

[1] R. B. Dingle, Proc. R. Soc. London, Ser. A **201**, 545 (1950).
[2] A. F. Mayadas and M. Shatzkes, Phys. Rev. B **1**, 1382 (1970).
[3] M. Barati and E. Sadeghi, Nanotechnology **12**, 277 (2001).
[4] Y.-M. Lin, X. Sun, and M. S. Dresselhaus, Phys. Rev. B **62**, 4610 (2000).
[5] S. B. Cronin, Y.-M. Lin, O. Rabin, M. R. Black, J. Y. Ying, M. S. Dresselhaus, P. L. Gai, J.-P. Minet, and J.-P. Issi, Nanotechnology **13**, 653 (2002).
[6] N. Garcia, Y. H. Kao, and M. Strongin, Phys. Rev. B **5**, 2029 (1972).
[7] V. P. Duggal and R. Rup, J. Appl. Phys. **40**, 492 (1969).
[8] M. R. Black, M. Padi, S. B. Cronin, Y.-M. Lin, O. Rabin, T. McClure, G. Dresselhaus, P. L. Hagelstein, and M. S. Dresselhaus, Appl. Phys. Lett. **77**, 4142 (2000).
[9] V. B. Sandormiskiĭ, Sov. Phys. JETP **25**, 101 (1967).
[10] T. W. Cornelius, M. E. Toimil-Molares, R. Neumann, G. Fahsold, R. Lovrincic, A. Pucci, and S. Karim, Appl. Phys. Lett. **88**, 103114 (2006).
[11] E. I. Rogacheva, S. N. Grigorov, O. N. Nashchekina, S. Lyubchenko, and M. S. Dresselhaus, Appl. Phys. Lett. **82**, 2628 (2003).
[12] K. Liu, C. L. Chien, P. C. Searson, and K. Yu-Shang, Appl. Phys. Lett. **73**, 1436 (1998).
[13] J. Heremans, C. M. Thrush, Y.-M. Lin, S. Cronin, Z. Zhang, M. S. Dresselhaus, and J. F. Mansfield, Phys. Rev. B **61**, 2921 (2000).
[14] X. F. Wang, J. Zhang, H. Z. Shi, Y. W. Wang, G. W. Meng, X. S. Peng, L. D. Zhang, and J. Fang, J. Appl. Phys. **89**, 3847 (2001).
[15] Z. B. Zhang, X. Sun, M. S. Dresselhaus, J. Y. Ying, and J. Heremans, Phys. Rev. B **61**, 4850 (2000).
[16] P. Chiu and I. Shih, Nanotechnology **15**, 1489 (2004).
[17] R. Spohr, German Patent No. DE 2951376 C2 (09/15/83); U.S. Patent No. 4,369,370 (01/18/83).
[18] T. W. Cornelius, J. Brötz, N. Chtanko, D. Dobrev, G. Miehe, R. Neumann, and M. E. Toimil Molares, Nanotechnology **16**, S246 (2005).
[19] M. E. Toimil Molares, N. Chtanko, T. W. Cornelius, D. Dobrev, I. Enculescu, R. H. Blick, and R. Neumann, Nanotechnology **15**, S201 (2004).
[20] T. W. Cornelius, M. E. Toimil-Molares, R. Neumann, and S. Karim, J. Appl. Phys. **100**, 114307 (2006).
[21] G. Pépy, P. Boesecke, A. Kuklin, E. Manceau, B. Schiedt, Z. Siwy, M. Toulemonde, and C. Trautmann, J. Appl. Crystallogr. **40**, s388 (2007).
[22] C. Schönenberger, B. M. I. van der Zande, L. G. J. Fokkink, M. Henny, C. Schmid, M. Krüger, A. Bachtold, R. Huber, H. Birk, and U. Staufer, J. Phys. Chem. B **101**, 5497 (1997).
[23] S. Farhangfar, Phys. Rev. B **74**, 205318 (2006).
[24] B. Lax, J. G. Mavroides, H. J. Zeiger, and R. J. Keyes, Phys. Rev. Lett. **5**, 241 (1960).
[25] M. R. Black, Y.-M. Lin, S. B. Cronin, O. Rabin, and M. S. Dresselhaus, Phys. Rev. B **65**, 195417 (2002).
[26] Yu. F. Komnik, E. I. Bukhshtab, Yu. V. Nikitin, and V. V. Andrievskii, Sov. Phys. JETP **33**, 364 (1971).